Species-specific traits mediate avian demographic responses under past climate change

Ryan R. Germain [1,2,18] ✉, **Shaohong Feng**[3,4,5,6,18], **Guangji Chen** [7,8],
Gary R. Graves [1,9], **Joseph A. Tobias** [10], **Carsten Rahbek** [1,10,11,12], **Fumin Lei** [13],
Jon Fjeldså[1,14], **Peter A. Hosner**[1,11,14], **M. Thomas P. Gilbert** [15,16],
Guojie Zhang [2,3,4,6,17] ✉ & **David Nogués-Bravo** [1] ✉

Anticipating species' responses to environmental change is a pressing mission in biodiversity conservation. Despite decades of research investigating how climate change may affect population sizes, historical context is lacking, and the traits that mediate demographic sensitivity to changing climate remain elusive. We use whole-genome sequence data to reconstruct the demographic histories of 263 bird species over the past million years and identify networks of interacting morphological and life history traits associated with changes in effective population size (N_e) in response to climate warming and cooling. Our results identify direct and indirect effects of key traits representing dispersal, reproduction and survival on long-term demographic responses to climate change, thereby highlighting traits most likely to influence population responses to ongoing climate warming.

Human-induced changes to the global environment are affecting biodiversity at an unprecedented rate, with animal populations having declined drastically since 1970 (refs. 1–4). Despite efforts to quantify contemporary population trends and disentangle the effects of different drivers of global change, we currently lack historical context as to whether similar declines have occurred before and whether species-specific traits influence long-term demographic sensitivity to environmental challenges such as climate change[5–7]. In particular, identifying common demographic patterns over evolutionary time scales, and before the Anthropocene epoch, can reveal how life history strategies influence population dynamics during periods of widespread climatic stress[8–10]. Explaining these strategies will aid conservation

[1]Center for Macroecology, Evolution, and Climate, The Globe Institute, University of Copenhagen, Copenhagen, Denmark. [2]Villum Centre for Biodiversity Genomics, Section for Ecology and Evolution, Department of Biology, University of Copenhagen, Copenhagen, Denmark. [3]Center for Evolutionary and Organismal Biology, Zhejiang University School of Medicine, Hangzhou, China. [4]Liangzhu Laboratory, Zhejiang University Medical Center, Hangzhou, China. [5]Department of General Surgery of Sir Run Run Shaw Hospital, Zhejiang University School of Medicine, Hangzhou, China. [6]Innovation Center of Yangtze River Delta, Zhejiang University, Hangzhou, China. [7]BGI Shenzhen, Shenzhen, China. [8]College of Life Sciences, University of Chinese Academy of Sciences, Beijing, China. [9]Department of Vertebrate Zoology, National Museum of Natural History, Smithsonian Institution, Washington, DC, USA. [10]Department of Life Sciences, Imperial College London, Ascot, UK. [11]Center for Global Mountain Biodiversity, The Globe Institute, University of Copenhagen, Copenhagen, Denmark. [12]Danish Institute for Advanced Study, University of Southern Denmark, Odense, Denmark. [13]Key Laboratory of Zoological Systematics and Evolution, Institute of Zoology, Chinese Academy of Sciences, Beijing, China. [14]Natural History Museum of Denmark, University of Copenhagen, Copenhagen, Denmark. [15]Center for Evolutionary Hologenomics, The Globe Institute, University of Copenhagen, Copenhagen, Denmark. [16]Department of Natural History, University Museum, Norwegian University of Science and Technology, Trondheim, Norway. [17]State Key Laboratory of Genetic Resources and Evolution, Kunming Institute of Zoology, Chinese Academy of Sciences, Kunming, China. [18]These authors contributed equally: Ryan R. Germain, Shaohong Feng. ✉e-mail: ryan.germain@bio.ku.dk; guojiezhang@zju.edu.cn; dnogues@sund.ku.dk

efforts through identifying species with characteristics prone to demographic decline under current and future challenges.

Climate change is regarded as a key environmental regulator of demographic change. It is proposed to affect demography via its effects on reproduction, survival and/or growth and dispersal[11,12]. However, responses to climate change can vary dramatically among even closely related or co-occurring species because of differing life history traits and strategies[13-15]. Theoretical predictions and empirical evidence suggest that larger-bodied, slower-reproducing species with limited dispersal capacity are more sensitive to sustained climate change (Supplementary Table 11) because of reduced adaptive potential and/or limited ability to exploit climate refugia. However, evaluation of the role of traits in demographic sensitivity to climate change is typically tested only with contemporary data over shorter ecological time scales. Because additional environmental stressors such as land use change and overexploitation may mask or confound demographic responses[9,16-18], the ability to identify relationships between life history traits and demographic sensitivity to climate change remains constrained when limited to contemporary data.

Periods of climate warming and cooling over the Earth's history offer a unique opportunity to quantify effects of species-specific traits on demographic sensitivity to climate change in the absence of confounding anthropogenic stressors[5,6]. We use whole-genome sequence (WGS) data[19] and pairwise sequential Markovian coalescent (PSMC) analysis[20] to reconstruct the long-term (roughly 1 million years) demographic histories of 263 bird species, representing 39 orders distributed from the poles to the tropics. We then quantify demographic responses to the most recent warming and cooling periods before widespread human activity and identify network effects of morphological and life history traits related to survival and/or growth, reproduction and dispersal that influence overall demographic sensitivity to climate change.

Results and discussion

Effective population sizes (N_e) varied substantially across avian species and over time and space (Supplementary Note 1 and Supplementary Table 1). Demographic clustering revealed seven main demographic patterns, inferred from temporal patterns of N_e over the past million years (Fig. 1 and Supplementary Table 3). Overall position of each species in the avian phylogeny did not explain the observed differences among demographic patterns (Supplementary Fig. 7). Passerines (order Passeriformes, which represent more than half of all extant bird species globally[21]; here $n = 123$ species) and Non-Passerines ($n = 140$ species) were unequally distributed among the demographic clusters ($X^2 = 23.81$, d.f. = 6, $P < 0.001$), where Passerines were most heavily represented in clusters 1, 3, 4 and 7 (that is, demographic peaks in the more recent Upper to Middle Pleistocene; Fig. 1 and Supplementary Table 3). In contrast, Non-Passerines were most represented in clusters 5, 6 and 7, depicting demographic peaks during the more ancient periods of the Middle and Lower Pleistocene (Fig. 1 and Supplementary Table 3). These results were further reflected in lower mean N_e values for Passerines in the more distant past, despite Passerines exhibiting consistently higher mean N_e than Non-Passerines over the past million years (Fig. 2a). Species currently classified as 'threatened' or 'near-threatened' (IUCN Red List; here $n = 34$ species) were evenly distributed among the seven main demographic patterns ($X^2 = 5.77$, d.f. = 6, $P = 0.45$) and exhibited varying demographic trends over time (Fig. 2b), indicating that current conservation status is unlikely to be the result of long-term demographic variation.

Globally, mean normalized N_e for all 263 species increased from 1 Mya to roughly 500–600 kya, after which it steadily declined (Fig. 3, 'global average'). Across the Earth's major zoogeographic realms (Supplementary Note 1), species differed only slightly in when they reached their mean demographic peaks. Most species followed similar patterns of higher mean N_e in more ancient periods and lower N_e values closer to 30 kya (Fig. 3), and there was little concordance between
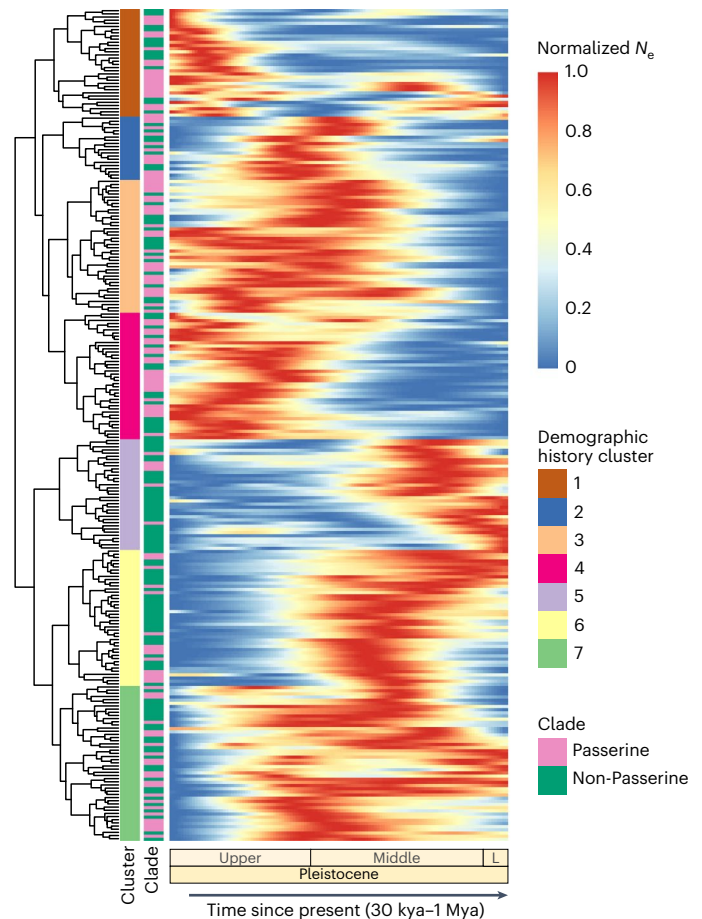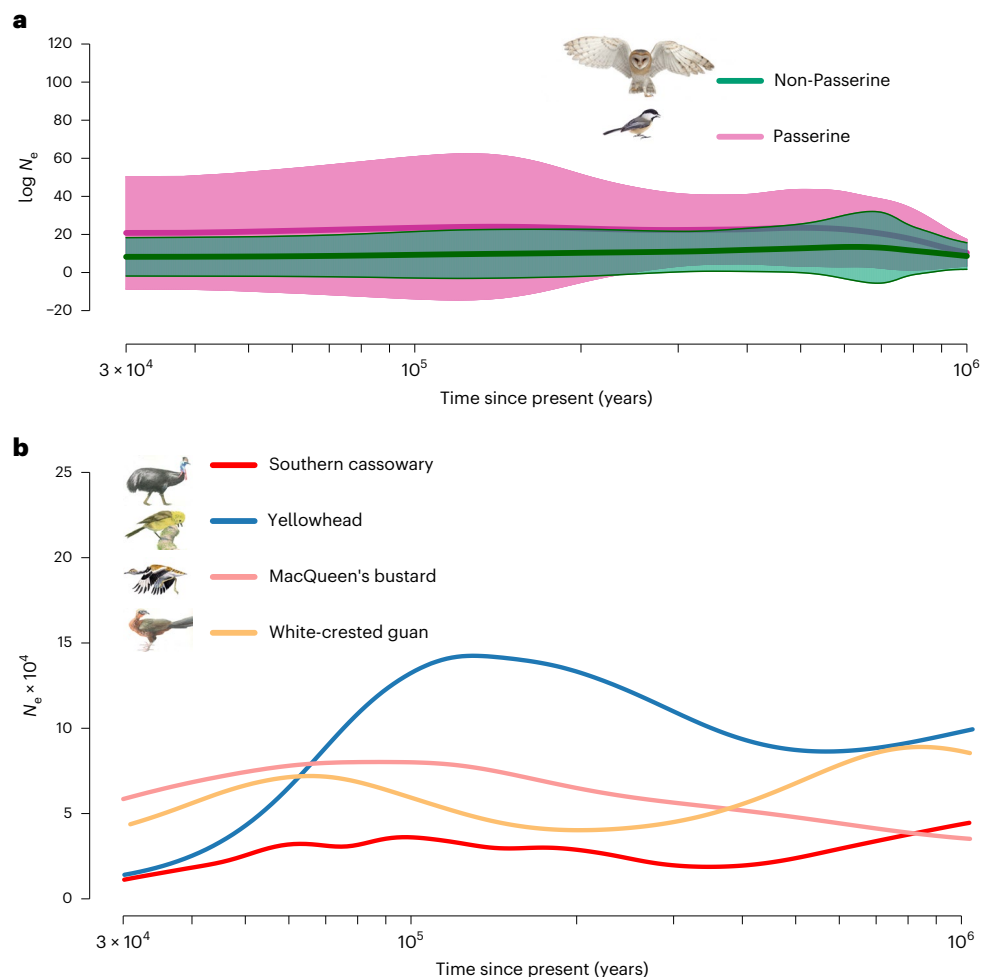

Fig. 1 | Demographic histories of 263 avian species from 30 thousand years ago (kya) to 1 million years ago (Mya) (*x* axis presented on the log₁₀ scale). Cluster analysis of normalized N_e values revealed seven main demographic patterns over the Upper/Middle/Lower (L) Pleistocene. Clusters designating groups 1–7 (see Supplementary Table 1 for species included in each group) were based on overall similarity of long-term N_e patterns but can be distinguished by when most species reached their relative peak (Supplementary Table 3).

geographic realm and allocation to a given demographic cluster group (Supplementary Fig. 21). Overall, we detected minimal variation in demographic trends among realms (Supplementary Fig. 22), indicating little effect of geographic variation on overall patterns of demographic change over time.

We used linear mixed-effect models (Gaussian distribution) to first identify the set of morphological and life history traits most likely to be associated with overall N_e dynamics in response to climate change, for use in downstream analyses (that is, those explicitly considering phylogenetic and trait interactions, below). For this variable selection step, we designated two periods of relatively recent warming (roughly 147–123 kya) and cooling (roughly 122–65 kya), which represent some of the most dramatic changes in global climate (that is, Δ of roughly 8 °C in global average surface temperature in less than 60,000 years) over the past million years (Supplementary Fig. 8), and are within the time window (roughly 30–200 kya) in which PSMC-based estimates of N_e are most precise[20]. We quantified demographic sensitivity to climate change as the relationship between species-specific N_e and global average surface temperature during these two periods via Pearson correlation coefficients, and designated these relationships as 'climate warming' and 'climate cooling' responses. Of eight initial traits (body mass, brain–body ratio, tarsus length, bill length, egg mass, clutch size, incubation duration and hand–wing index (HWI, a metric of dispersal ability)) expected to influence these estimates of

Fig. 2 | Demographic histories of different avian groups from 30 kya to 1 Mya (all x axes presented on the $\log_{10}$ scale). a, Mean $\log N_e$ values (±s.d.) of Passerine and Non-Passerine species. Passerines exhibited consistently higher N_e values (mean sample difference 9.21) across 120 equally spaced (log linear) time points from 30 kya to 1 Mya (paired two-sided t-test, $t_{119} = 27.9$, $P = 2.2 \times 10^{-16}$). **b**, Examples of differing demographic histories of species currently designated as 'threatened' under IUCN Red List status, where species arriving at similar N_e values at roughly 30 kya follow differing demographic patterns over time (illustrations by J.F.).

demographic sensitivity to climate change (Supplementary Note 2), six were identified as key potential influencers (that is, retained in a subset of 'best-fitting' models, Table 1) for climate warming and/or climate cooling responses, and retained in subsequent analysis. Of these six traits, longer incubation durations and larger clutch sizes were most closely associated with increasing N_e during climate warming, whereas shorter incubation duration, lower HWI and longer bill lengths were most closely associated with increasing N_e during climate cooling (Table 1). While goodness of fit for these models were low ($R^2 = 0.06$, 0.05), given the low expectation of variation in a single trait directly influencing N_e responses to climate over evolutionary time scales[22], these results reveal the suite of key traits among our initial candidate traits that are most likely to be associated with long-term demographic variation under climate change.

Using these six key traits, we further characterize the phylogenetically explicit interacting trait network of influences on demographic sensitivity to climate change. We categorized each species by their combined climate warming and climate cooling responses and used phylogenetic path analysis (PPA). PPA is a hypothesis-driven framework for assessing direct and indirect effects of each trait on differentiating defined species categories, independent of their phylogenetic relationships (Supplementary Fig. 10). Species exhibiting decreasing N_e under climate cooling and increasing N_e under climate warming

were categorized as 'warming positive' (Fig. 4 and Supplementary Table 5). Those exhibiting increasing N_e under climate cooling and decreasing N_e under climate warming were categorized as 'warming negative', a scenario expected for many temperate and cold-adapted species during the twenty-first century. We quantified the network of trait effects on differentiating warming positive species from all other species in our analysis, and repeated this process for warming negative species. Further, we evaluated species that exhibited overall sensitivity to climate warming or cooling (that is, warming positive + warming negative responses, hereafter 'climate sensitive') versus those with consistent N_e increases or decreases, and those that exhibited consistent decreases in N_e for both the climate warming and climate cooling responses (categorized as 'consistent N_e decrease') versus remaining species (Supplementary Table 5).

PPA revealed that warming positive species were best differentiated by direct effects of reproductive, survival and/or growth and dispersal traits (Supplementary Table 6 and Core Model D in Supplementary Fig. 10). Averaging the best-performing models from this comparison indicates that N_e of species with larger body masses, lower HWI, and smaller egg masses were more likely to increase under climate warming and decrease under climate cooling (Fig. 4a). Body mass also had indirect effects on differentiating warming positive species from remaining species via its significant positive influence
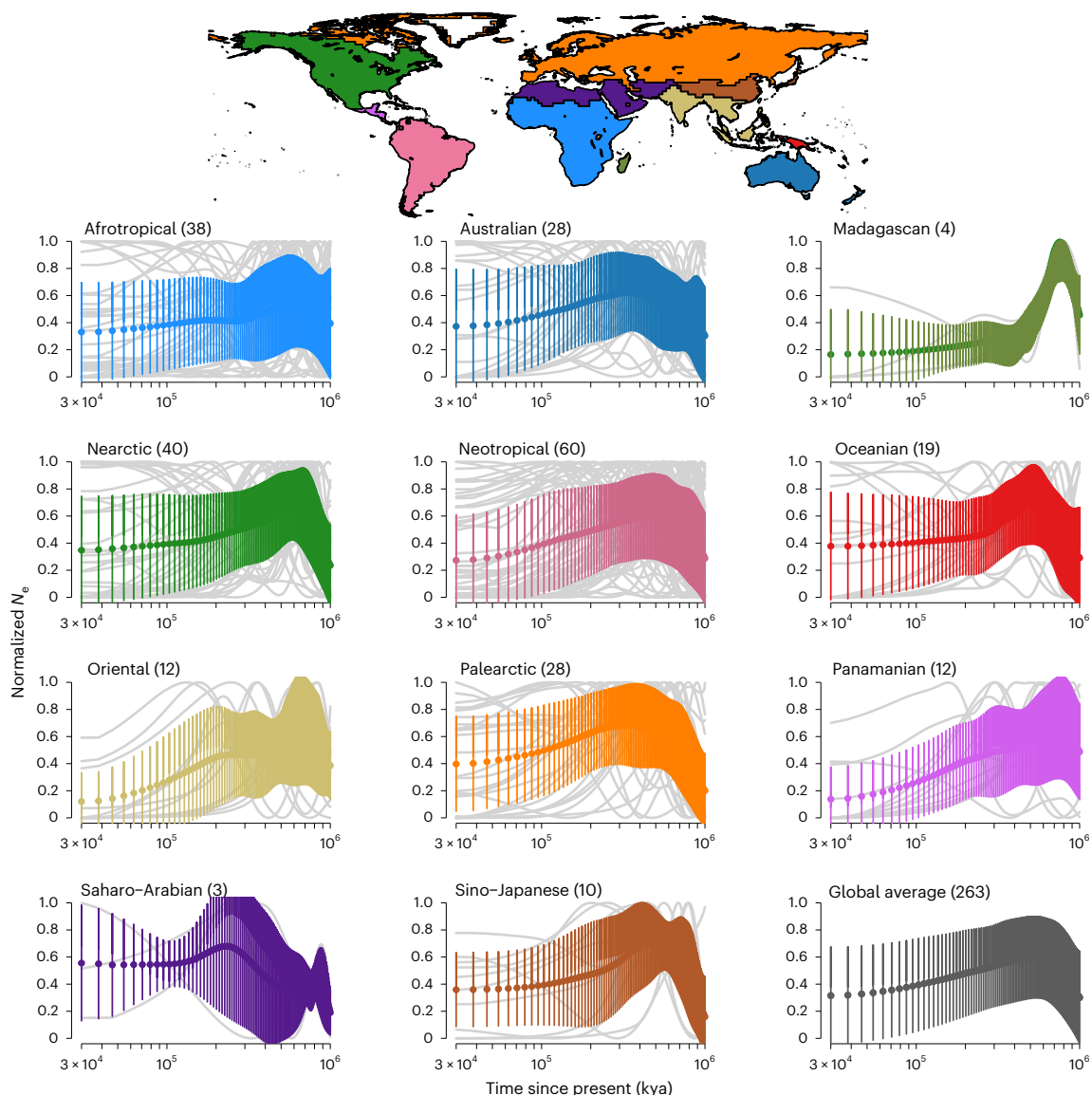
Fig. 3 | Mean change in normalized N_e from 30 kya to 1 Mya for 263 avian species, summarized by zoogeographic realm. For each panel, the number of species representing each realm is given in parentheses. Coloured dots depict mean normalized N_e at 120 equally spaced (log linear) time points from 30 kya to 1 Mya, while the shaded area depicts s.d. at each point. Full demographic curves of each species are provided in the background (grey) to show overall variation within each realm. Top: Zoogeographic realms following Holt et al.[59].

on egg mass and its indirect correlation with a lower HWI (Fig. 4a). These results highlight potential trade-offs between the influences of reproductive, survival and growth and dispersal traits on changes in population size under climate warming, where the positive effects of larger body mass are offset by the associated increase in egg mass or decrease in HWI. Warming negative species were also best differentiated via the direct effects of reproductive, survival and/or growth and dispersal traits, but in the opposite directions compared with what we found in warming positive species (Supplementary Table 6 and Core Model D in Supplementary Fig. 10). Model averaging further revealed that smaller-bodied species with larger eggs, longer incubation durations and greater HWI were more likely to exhibit decreasing N_e under climate warming and increasing N_e under climate cooling, and again highlighted potential trade-offs between body mass and HWI (Fig. 4b). Trait-network effects on differentiating all climate sensitive species were less defined, where no traits were found to have significant, direct effects on differentiating both warming positive and warming negative species from remaining species (Fig. 4c). However,

species with consistently decreasing N_e tendency for both the climate warming and climate cooling responses were differentiated by smaller clutch sizes and tended to have shorter incubation durations than remaining species (Fig. 4d), providing additional evidence for the directional role of these key traits in mediating demographic responses under climate change.

Our observations of trait-network influences on long-term demographic sensitivity to climate change agree with theoretical expectations that larger-bodied, slower-reproducing species with limited dispersal capacity are likely to respond strongly to changing climate (Fig. 4). However, they also suggest that such traits may not necessarily lead to population declines under warming climate conditions as predicted from some empirical observations in contemporary populations[12,13,15,23–25] (Supplementary Table 11). A lower HWI typical of species with limited dispersal ability was the only predictor found to significantly influence both un-networked (Table 1) and networked (Fig. 4a,b) responses to climate change, where such species tended to increase in abundance under climate cooling and decrease under climate warming.

Table 1 | Parameter estimates, standard errors (s.e.) and upper and lower 95% confidence intervals (UCI, LCI) from averaged two-sided linear mixed models (random effect equal to Passerine/Non-Passerine) evaluating the relative effects of morphological and life history traits on demographic responses to climate warming and cooling (measured as correlation coefficient between N_e change and climate change)

	Estimate	s.e.	z value	P	LCI	UCI
Climate warming (R^2=0.06)						
Intercept	0.0003	0.07				
Incubation duration	0.15	0.08	1.92	0.06	−0.003	0.30
Clutch size	0.13	0.07	1.91	0.06	−0.004	0.27
Egg mass	0.12	0.08	1.61	0.11	−0.03	0.27
HWI	−0.09	0.07	1.34	0.18	−0.22	0.04
Body mass	0.05	0.07	0.82	0.41	−0.08	0.19
Climate cooling (R^2=0.05)						
Intercept	−0.0005	0.08				
Incubation duration	−0.14	0.07	1.93	0.05	−0.28	0.002
HWI	−0.14	0.07	2.00	**0.05**	**−0.28**	**−0.003**
Bill length	0.05	0.07	0.70	0.49	−0.09	0.18

Values marked in bold highlight statistically significant predictors (that is, confidence intervals do not overlap zero). For each response, we ran 256 models involving all possible combinations of eight predictor variables (body mass in g, ratio of brain size to body mass, tarsus length in mm, HWI, bill length in mm, egg mass in g, incubation duration in days and clutch size; all z scaled to remove the effects of measurement scale), selected a 'best models' subset (ΔAIC ≤ 5 from the best-fitting model) and averaged parameter estimates within this subset. R^2 represents the goodness of fit of the global model (including all explanatory variables) for each response.

We further found that larger body mass had direct and indirect effects on increasing N_e under climate warming and decreasing N_e under climate cooling (Fig. 4a,b), contrary to results from contemporary studies (that is, over ecological time scales, Supplementary Table 11). Such differences are probably due to the much longer (evolutionary) time scales investigated here via our PSMC analysis (below).

If morphological and life history traits play a central role in demographic responses to climate change, as determined from our historical N_e analyses, they may also be reflected in the contemporary global distributions of species. Specifically, trait effects leading to an increasing N_e trend under the climate warming period may be similar to those of species found in tropical locations today, under the assumption that such species are adapted to warmer climates. Using all available mean trait and breeding and resident range information for 2,745 avian species sampled from around the world, we found that species in tropical latitudes tend to have longer incubation durations and longer bills, but smaller clutch sizes, smaller eggs, lower HWIs and lower body mass (Supplementary Note 3 and Supplementary Figs. 23 and 24). Thus, our findings of historical responses to periods of climate warming do partially explain contemporary biodiversity patterns. Specifically, tropical species exhibit lower HWIs, in concordance with species exhibiting such traits showing increasing N_e trends under climate warming (Supplementary Figs. 11e and 12e). However, the opposing findings of smaller clutch sizes among tropical species and the tendency towards larger clutch sizes among climate warming responses (averaged model, Supplementary Fig. 12e), as well as the remaining traits having no significant direct effect among climate warming responses, indicate that historical responses to climate change alone are only partially predictive of contemporary distributions.

Our study reveals seven main demographic patterns among a broad geographic (Fig. 3) and phylogenetic (Supplementary Fig. 7) sample of birds over the past million years, and a key trait-adaptive network associated with population responses to long-term climate change in the absence of additional human effects. Unlike short-term responses to climate change (for example, studies listed in Supplementary Table 11) where single traits dictate adaptive functions under strong natural selection[12,15], long-term adaptation (that is, over evolutionary time scales) is influenced by overall genomic variation within species, where the effects of individual traits become saturated and diminish over

time[22,23,26,27]. This is reflected both in the very low goodness of fit associated with individual trait effects (that is, un-networked) models (Table 1) and in trade-offs among several traits in PPA analysis of responses to periods of climate warming and cooling (Fig. 4 and Supplementary Figs. 11 and 12). Over hundreds of thousands of years, interacting trait networks and trade-offs among survival and/or growth and reproductive traits may develop that potentially mask direct trait effects identified in studies of contemporary populations. Reconstructing long-term population dynamics from genomic data is thus a crucial component of revealing how past climatic events influenced the genetic makeup of contemporary populations over time, and for providing demographic baselines before the Anthropocene[5,6]. Such analyses across the tree of life will provide unique insight into the natural variability of long-term demography, and help direct conservation efforts towards species more sensitive to broad-scale global environmental change.

Methods

SNP calling and mutation rate estimation

WGS data for 345 bird species were collected by Feng et al.[19] and released as genomic resources of the Bird 10,000 Genomes (B10K) Project Phase II (https://b10k.genomics.cn). Genomes for each species were generated under a standardized protocol of library building, sequencing and assembly as part of this previous study, thereby minimizing potential bioinformatic artefacts that could affect our analyses and interpretations. We inferred heterozygous information of each species using BWA + GATK pipeline[20,28]. Four filtering steps were applied to obtain high-quality single-nucleotide polymorphisms (SNPs)[29]: (1) removing homozygous SNPs (that is, those where the genotype was encoded as 'Minor/Minor' in the variant call format file) and SNPs with more than two alternative alleles, (2) removing SNPs with an interval below 10 bp, (3) removing SNPs with a read depth below one-third or over twice the average read depth across the genome and (4) removing SNPs with a root-mean-square mapping quality lower than 25.

We used branch-specific estimates of the substitution rate per site (*R*) from a dated phylogeny provided by the latest B10K family-phase phylogenetic study as proxies for mutation rate (*μ*). This latest topology was inferred based on WGS data of 363 species, assumed to be the most effective in addressing deep evolutionary relationships[30–32]. Divergence
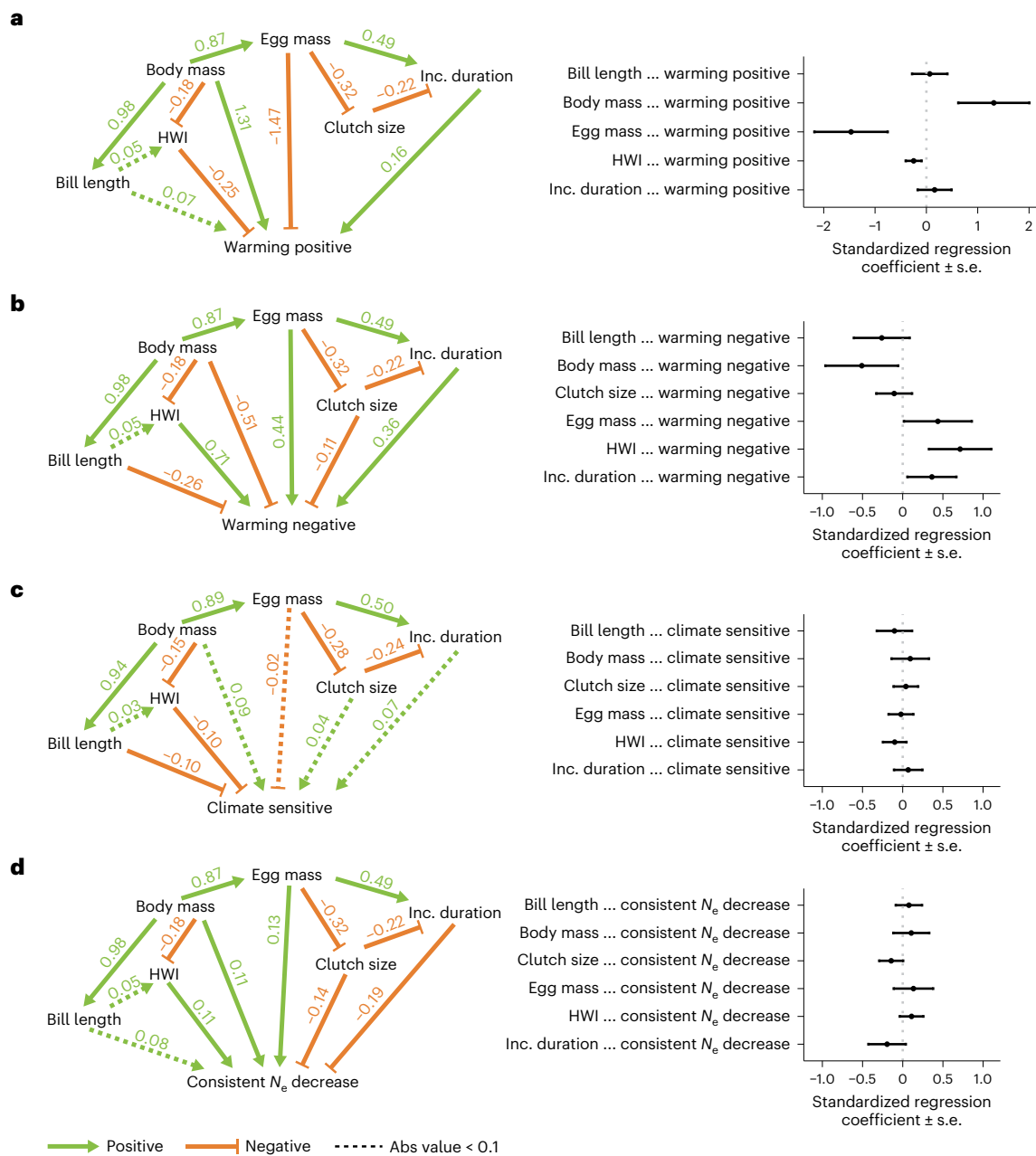
Fig. 4 | Network effects of key morphological and life history traits on demographic responses to climate warming and climate cooling, shown as directed acyclic graphs (left) and corresponding standardized regression coefficients (±s.e.) (right) for averaged best-performing models. **a**, Comparison of warming positive responses (n = 33) versus all remaining species (n = 230) reveals that larger body masses, smaller egg masses and lower HWI are associated with demographic increases during climate warming and decreases during climate cooling (statistical significance of trait effects in all panels assessed by whether s.e.s overlap zero). **b**, Comparison of warming negative responses (n = 29) versus all remaining species (n = 234) reveals that smaller body masses, larger egg masses, greater HWI and longer incubation (Inc.) durations

are significantly associated with demographic increases during climate cooling and decreases during climate warming. **c**, Comparison of all species that exhibited sensitivity to climate warming or cooling (n = 33 + 29) versus those with consistent N_e increases or decreases (n = 98 + 55) reveals no traits significantly influenced overall species sensitivity to changing climate conditions. **d**, Comparison of species with consistent N_e decreases during climate warming and climate cooling (n = 98) versus all remaining species (n = 165) again reveals no significant influences, although species with smaller clutch sizes, higher HWI and shorter incubation durations did tend to exhibit demographic decrease during both climate warming and climate cooling. For all left panels, dashed lines represent standardized regression coefficients with an absolute (Abs) value < 0.1.

times (*t*) were estimated by MCMCTree[33] with a large number of fossil records to provide by far the best calibration information[34,35]. Both of these measures ensure the highest-possible accuracy of species-specific substitution estimates, as well as divergence times. To further convert the unit of mutation rate from per site to per site per generation, we scaled the species-specific mutation rates (*μ*) as $\mu = \frac{R}{t} \times T$, where *T* is the generation time for each species.

Demographic reconstruction over the last million years

We used the PSMC method[20] to reconstruct long-term changes in N_e for each species. Diploid genomes consist of thousands of independent loci; the coalescent approach underlying PSMC estimates the time to the most recent common ancestor of the two alleles at each locus, creating an overall the most recent common ancestor distribution across the genome. The rate of coalescent events is inversely

proportion to N_e, therefore the PSMC method can identify periods of changing N_e over time (for example, if many loci were observed to coalescent at a given time point, it would indicate a lower N_e at that time)[20]. To ensure reliability of PSMC analyses, we removed 20 species with lower-quality heterozygosity information (that is, less than 18× genome-wide coverage or more than 25% missing data, as recommended by Nadachowska-Brzyska et al.[36]). For the remaining 325 qualified species (Supplementary Table 1), we used the PSMC settings '-N30 -t5 -r5 -p 4 + 251*1 + 4 + 6 + 10' with a reduced dataset, and then scaled results to real time using estimated mutation rate (above) and generation time[37]. This set of parameters had an increased number of free atomic intervals (-p) on the basis of previous study[29], which could generate more PSMC estimates without changing the shape of the PSMC curves (Supplementary Fig. 1). Data representing N_e estimates (×10^4) scaled to real time via PSMC for all 325 species are available online[38]. Because recent and drastic population bottlenecks, and associated severe inbreeding, can lower PSMC-based estimates of N_e in more recent time periods and erase information regarding ancient N_e dynamics, we restricted downstream analyses to the 263 species with full demographic coverage over the focal time period (30 kya–1 Mya) for which we had the most confidence in PSMC-based estimates of effective population size. Of the 62 species excluded via this step for which conservation status was available, 19 are currently listed as 'threatened' or 'near-threatened' (IUCN Red List; www.iucnredlist.org), indicating a tendency ($X^2 = 10.78$, $P = 0.001$) towards such species to have limited polymorphism information needed to quantify long-term demographic history, once again probably due to recent population bottlenecks.

Since its initial development[20], the PSMC method has been widely applied across taxa to detect changes in N_e on the basis of WGS information. Because PSMC does not rely on population data and can straightforwardly construct historical N_e dynamics over time, it is favoured among de novo genome projects for its accuracy and precision[39], particularly regarding demographic changes in the more distant past[40–43]. Although there are some generally accepted filtering strategies for sequence data to improve the accuracy of demographic reconstructions[36], potential biases in PSMC output can be the result of both scaling parameters (for example, mutation rate) and population structure. For the former type, changes in the scaling parameters cause the PSMC curve to move along the axes while maintaining the overall curve shape[29]. To account for this, we performed a robustness test of the PSMC curves in terms of sampling mutation rates from the posterior distributions on a dated phylogenetic tree (below, Supplementary Fig. 1). For the later type of bias, theoretical work has shown that the accuracy and interpretation of PSMC results can be affected by population structure, in that changes in connectivity among subpopulations may influence overall patterns of demographic change[44–46]. While we have no a priori information on changes in connectivity over the last million years for our 263 species, we assume that the patterns observed are probably the result of a combination of changes in both population size and a degree of changes in population connectivity, both of which would be mediated by the effects of trait networks under periods of climate change (that is, species with stronger dispersal ability (HWI) maintaining greater connectivity during periods of extreme environmental change). Thus, while not infallible, our analyses and results present a key step forwards in our understanding of how trait networks can mediate demographic responses to periods of acute climate warming and cooling over the past million years.

Cluster analysis of demographic patterns and robustness tests
To investigate patterns in overall demographic fluctuations among the 263 bird species, we applied clustering analysis based on normalized N_e values. We first selected 121 time points with equal time intervals (after log$_{10}$ transformation) from 30 kya to 1 Mya. For each species, we extracted the corresponding N_e values for these 121 time points along

the species-specific N_e trajectory and used min-max normalization to rescale values between 0 and 1. These normalized N_e values resulted in a 263 × 121 matrix, which was then used as the input for a hierarchical clustering analysis based on the Euclidean distance performed in pheatmap (with 'cluster_row = T'). Clustering methods aim to define clusters such that the total intragroup variation is minimized. In this instance (for example, Fig. 1), species with similar N_e trajectories are found closer together on the clustering dendrogram. To summarize the major demographic patterns among species for the past million years, we used the 'cutree' function in the R package dendextend[47] to split the resulting clustering dendrogram into 3, 4, 5, 6 and 7 groups (that is, $k = 3$–7), respectively (Supplementary Figs. 2–5). Compared with a lower value of k (for example, $k = 3$, Supplementary Fig. 2), dividing the dendrogram into $k = 7$ subtrees (Fig. 1) made the species contained in each subtree more compact in terms of N_e pattern consistency and was sufficient to clearly identify the major fluctuation patterns.

Different methods of data transformation can lead to different interpretations of both the appropriate number and organization of clusters. The minimum and/or maximum normalization approach used here focuses on the mode of demographic fluctuations, whereas other methods (for example, rescaling the mean) take into account both the mode and degrees of change. Because our analyses centre on the positive versus negative relationships between demographic change and climate change during periods of warming and cooling, our normalization method should likewise focus on the modes of positive or negative demographic responses, rather than the degrees of change. However, to examine the robustness of our clustering analysis to the choice of data transformation, we used the 'TreeDistance' function in the R package TreeDist[48] to calculate the distance (0–1, where higher values indicate more similarity) between the output clustering trees generated after the minimum and/or maximum normalization approach and three other data transformation methods (rescaling the mean, Z transformation and coefficient of variation). The distance value between the minimum and/or maximum normalization normalization and Z transformation was 0.83, and the distance value between the minimum and/or maximum normalization normalization and the coefficient of variation was 0.82, indicating that the cluster designations from these three separate methods were relatively consistent. While the distance value between minimum and/or maximum normalization normalization and rescaling the mean was relatively lower (0.66), indicating less consistency between clustering results, this was expected given the points made above (rescaling being based on combining the modes and degrees of fluctuations). We further used Rezende's 'phylo.signal.disc' algorithm[49] to examine the phylogenetic signal underlying cluster designations from these four data transformation methods (see below for full results from minimum and/or maximum normalization normalization). For rescaling the mean, the observed number of transitions was 153, which was not significantly different from what was expected by chance (randomized mean transitions 154, $P = 0.46$), indicating that phylogeny alone did not explain the observed differences among demographic patterns. Similarly, observed transitions for the Z transformation and coefficient of variation methods did not significantly differ from chance ($P = 0.21$ and 0.99, respectively). Thus, in terms of phylogenetic signal testing, all alternative normalization methods investigated returned consistent results and conclusions to the minimum and maximum normalization we used throughout our analyses.

Considering that transforming PSMC outputs into real time is sensitive to the value of mutation rates[20], we let the species-specific mutation rates vary within a reasonable range to generate random input matrixes and assess the robustness of the above clustering result. As a time-estimation algorithm based on Bayesian theory, MCMCTree provides the posterior age distributions for each node[33]. Therefore, we first randomly sampled 100 estimates of the divergence time from the posterior distribution of nodes corresponding to each species.

With the fixed substitution rates and generation times, 100 mutation rates were calculated for each species using these random values on the basis of the formulas provided above and then used to scale the PSMC output from the coalescent unit to the real time unit. This gave 100 N_e trajectories per species on the basis of varying mutation rates. Next, we randomly selected one of these trajectories from each species and extracted the same 121 time points as before to form a new 263×121 matrix. This step was repeated 100 times and the resulting 100 matrixes were next used to produce the clustering results, as well as the split results under different number of groups (k). When $k = 7$, we first randomly selected 500 pairs of species and obtained the information on whether each pair of species belonged to the same group in the clustering dendrogram shown in Fig. 1. Then, for the same pair of species, we checked how many times the clustering results obtained from 100 random matrixes are consistent with the Fig. 1 clustering dendrogram, in terms of the group information. For example, species A and species B were from the same group in Fig. 1, and they were also considered to be from the same group in 100 random clustering results. The consistency ratio for these two species was then calculated as a percentage. The average consistency ratio for all 500 pairs of species was used to represent the robustness value for $k = 7$, and we repeated this process for all other k values (Supplementary Table 2). Robustness values increased with the number of clustering groups used, and was 83.49% when $k = 7$. A higher k value indicates higher intragroup similarity and lower intergroup similarity. Thus, a pair of species from the same group at $k = 7$ is more likely to have the sufficient similarity of N_e trajectories to be clustered together even when there is some estimation bias in the mutation rate, compared with species from the same group at $k = 4$. Given that the major fluctuation patterns are identified and the robustness is over 80% at $k = 7$, we used splitting results from this grouping number in subsequent analysis (Fig. 1).

We next ran a Chi-square test to examine whether the splitting pattern for $k = 7$ could be explained in part by when species within each cluster group reached their maximum effective population size (here, normalized N_e value greater than 0.9 is considered as a maximum value; Supplementary Table 3). Compared with expected background patterns, the N_e fluctuations of species in groups 1, 3 and 4 tended to reach their maximums during the Upper Pleistocene (30–129 kya), while those of groups 6 and 7 reached their maximums in the Middle Pleistocene (129–774 kya) and those of species in group 5 reached their maximums during the Middle and Lower Pleistocene (774 kya–1 Mya; Supplementary Table 3). Unlike these groups, group 2 did not show significant differences from expected background patterns during any of the time periods. To further determine the association between clustering and mean effective population size, we averaged N_e values over 30 kya–1 Mya for each species and quantified intra- and intergroup differences (analysis of variance) on the basis of the $k = 7$ clustering groups. From these comparisons, we detected significant differences in mean N_e between groups 5 and 1 and between groups 5 and 3, where individuals clustered in group 5 had lower mean N_e over time than those in groups 1 and 3, but where all other pairwise comparisons revealed no significant differences in mean N_e over time (Supplementary Fig. 6).

To analyse how lineages may resemble each other in overall demographic fluctuations (that is, whether phylogenetically related species are classified into the same cluster groups), we used Rezende's 'phylo. signal.disc' algorithm[49]. This algorithm compares the minimum number of character-state transitions at each node that account for the observed character distribution in the phylogeny, assuming maximum parsimony with the median of a randomized distribution (1,000 randomizations were used). If the observed evolutionary transitions are significantly less than the randomized median, a phylogenetic signal is inferred. The observed transitions were 171 when $k = 7$, which were not significantly lower than expected by chance (the randomized median transitions were 175, $P = 0.21$, Supplementary Fig. 7a). Even when some phylogenetically related lineages were observed to have similar N_e

trajectories under $k = 4$ (red background in Supplementary Fig. 7b), the similarities were still not significant (observed transitions 123, randomized median transitions 128, $P = 0.13$; Supplementary Fig. 7b). These results indicates that there are factors other than phylogeny that contribute to the convergent patterns of demographic fluctuations.

Quantifying demographic responses to recent periods of climate warming and cooling

The last one million years of the Earth's history is punctuated by periods of abrupt climate warming and cooling[50], the most dramatic of which have occurred in relatively recent paleo-ecological time (cooling from roughly 122–65 kya; warming from roughly 147–123 kya; Supplementary Fig. 8). Such periods of more recent paleo-ecological time also correspond to when PSMC-based estimates of N_e provide more detailed representations of demographic fluctuations within a defined window of time, and thus allow for the most accurate quantification of the relationship between climate change and changing N_e for each species.

To quantify the effects of climate warming and cooling on species-specific demographic trends over time, we first obtained the real time points and N_e values scaled from PSMC estimates for each individual within these two climate periods, and inferred the climate values for these time points from Snyder[50]. Snyder[50] presented climate data over the last million years (and beyond; estimated from a spatially weighted, multi-proxy database of more than 20,000 sea surface temperature reconstructions) as the change in global average surface temperature (one value 1,000 years), for example −6.12 in 65 kya and −5.99 in 66 kya. Thus, we could infer the climate value corresponding to any time point between two adjacent time points on the basis of the slope of the line between them. For example, on the basis of the above values, the climate value of 65.70 kya is calculated as −6.029. We then quantified overall N_e responses to warming and cooling (hereafter designated 'climate warming' and 'climate cooling') via Pearson correlation coefficients for two variables: N_e estimate and climate value. Following David[51], the recommend sample size for running Pearson's r is 25, or higher. In our study, the sample size is the number of corresponding N_e estimates and climate values for each individual during climate warming or climate cooling. Under the PSMC settings '-N30 -t5 -r5 -p 4 + 251*1 + 4 + 6 + 10', the average sample size in climate cooling was 26.91, while climate warming only contained 8.60 N_e estimates in average due to a shorter period. To avoid the under-powered calculations caused by such a small sample size in climate warming, we reran the PSMC analysis with the settings '-N30 -t5 -r5 -p 4 + 800*1 + 4 + 6 + 10'. These modified parameter settings allowed us to increase the average number of samples to 26.03 in climate warming, without changing the shape of the PSMC curves (Supplementary Fig. 1). In addition, we used 0.55 as the threshold for correlation coefficient to indicate statistical significance of a correlation, on the basis of the algorithm described by Guenther[52] with a power of 80%, alpha at 0.05 and sample size of 25. Guenther's algorithm also allowed us to determine whether the correlation coefficients calculated for individuals with sample sizes less than 25 were significantly different from zero. If the sample size of such species is smaller than the minimum sample size estimated from its correlation coefficient based on Guenther's algorithm, we consider this correlation coefficient to be 0. For example, the minimum sample size is 13 for Pearson's $r = 0.7$, when power was 80% and alpha was 0.05. Therefore, if there were only ten N_e estimates for a species, we cannot accept the correlation between N_e estimates and climate values even if its Pearson's r was as high as 0.7. After passing the above criteria, a positive correlation (at $P < 0.05$) corresponded to N_e tendency tracking changing temperature (that is, increasing N_e under increasing temperature or decreasing N_e under decreasing temperature). All significant positive and/or negative correlations were visually inspected to ensure they represented a predominantly linear relationship. The above analysis criteria are outlined visually in Supplementary Fig. 9.

To test the robustness of our estimated demographic responses to climate change, we randomly generated 1,000 mutation rates for each individual using the same strategy as the clustering robustness analysis (above). This gave 1,000 N_e trajectories per species on the basis of changes in mutation rates. By using the same quantitative criteria as our observed response results (Supplementary Fig. 9), we further assigned response labels to the estimated 1,000 trajectories per individual during the climate warming and climate cooling periods, respectively. On the basis of these response labels, we used the confidence level to represent the robustness, which is the percentage of response labels obtained from 1,000 random sampling events that are consistent with the observed response results for each individual. For example, for a species exhibiting a positive correlation in our observed results, if its response labels inferred from the random sampling were 950 positives and 50 negatives, its confidence level was 0.95. In summary, the mean confidence level is 0.90 during climate warming, and 0.92 during climate cooling, which indicated strong confidence in our observed demographic response estimates. Three types of demographic response ('increase', 'decrease' and 'unrelated'; determined by the strength of positive and/or negative correlations at different confidence levels) are summarized in Supplementary Table 4.

For later inclusion in PPA (below), we categorized each species by their combined climate warming and climate cooling responses. Species that exhibited decreasing N_e under climate cooling and increasing N_e under climate warming were categorized as warming positive ($n = 33$), while those with the opposite response (N_e increase under climate cooling and decrease under climate warming) were categorized as warming negative ($n = 29$; Supplementary Table 5). There were 48 species where demographic change was not correlated with changing temperature during either climate warming or climate cooling (categorized as 'N_e independent of climate change'). The remaining 153 species either showed consistent N_e increases under both climate warming and climate cooling ($n = 55$), or consistent N_e decreases under both these periods of climate change ($n = 98$; Supplementary Table 5).

Quantifying the relative influence of individual traits on population responses to climate change

We used linear mixed-effect models (Gaussian distribution) and multi-model inference via the lme4 (ref. [53]) and MuMIn[54] R packages as a variable selection step to identify the set of morphological and life history traits most likely to be associated with population responses during the periods of climate warming and climate cooling (on the basis of Pearson correlation coefficients, above). For each response variable, we constructed a set of models with Passerine or Non-Passerine as a random effect to account for Passerines exhibiting both greater mean and greater variance in N_e values across the full study period (Fig. 2a), since we aimed to identify traits linked to demographic responses to climate change while reducing the potential effects of broad-scale phylogenetic signal on such results ('PPA to identify trait-network effects on demographic responses to climate change' below). Each global (that is, all variables included) model also included eight non-collinear morphological/life history traits predicted to influence population responses to climate change (Supplementary Note 2) as fixed effects. These eight traits (selected from an initial set of 17 candidate traits, Supplementary Table 11) were: mean unsexed mass or mean of male and female masses (g, 'body mass'), ratio of brain size to body mass ('brain–body ratio'), mean unsexed tarsus length or mean of male and female tarsus length (mm, 'tarsus length'), mean unsexed bill length or mean of male and female bill length (mm of total exposed culmen, 'bill length'), mean mass of fresh eggs (g, 'egg mass'), mean number of eggs per clutch ('clutch size'), duration of clutch incubation (days, 'incubation duration') and 'HWI', measured as Kipp's distance (distance in mm between the tip of the first secondary feather to the tip of the longest primary feather) divided by total wing chord length (length in mm from bend of the wing to the longest primary of the unflattened

wing) and multiplied by 100. All fixed effects were standardized to mean of 0, s.d. of 1 to reduce potential influence of measurement scale on results and to allow direct comparison of model coefficients[55]. We further confirmed key model structure assumptions of homogeneity of variance (residuals versus predicted values) and normal distribution of residuals (QQ plots) for each global model. Goodness of fit (R^2) for each model was assessed by the conditional coefficient of determination[56]. We then ran $n = 256$ models for all possible combinations of these eight fixed effects for each response variable (correlation coefficient during climate warming and climate cooling, respectively) and selected a subset with a difference in Akaike information criterion (ΔAIC) ≤ 5 from the best-fitting model. For each response variable, we then averaged parameter estimates for each predictor included in this subset of models to create one representative (full-average) estimate of the relative effects of each component on N_e responses to climate warming and N_e responses to climate cooling (Table 1). Statistical significance for each fixed effect was assessed by whether 95% confidence intervals overlapped zero.

PPA to identify trait-network effects on demographic responses to climate change

We implemented the hypothesis-driven framework of PPA (phylopath R package[57]) to quantify the network of direct and indirect effects of key morphological or life history traits (identified via multi-model inference; above) on demographic responses to climate change while accounting for phylogenetic non-independence of species. PPA allows for a large number of models with complex configurations and intercorrelation of variables. In our study, six continuous variables representing our key morphological or life history traits (egg mass, clutch size, incubation duration, body mass, bill length and HWI) and one binary variable representing differing demographic responses to climate change (below) were included in each model. A total of 14 core models with different configurations of these variables were evaluated for each of our four comparisons using both P values and the C statistic information criterion (CICc) corrected for small sample sizes (Supplementary Fig. 10). Models were designed to test all possible networks of the traits and their effects on the demographic responses. Since the 'Reproduction' category contained three traits (egg mass, clutch size and incubation duration), core models assuming a direct effect of 'Reproduction' on demographic responses in fact have seven derived models (that is, at least one of the three traits having a direct effect on the demographic responses; Supplementary Fig. 10). The same is true for the 'survival and/or growth' category with two traits (body mass and bill length). Thus, depending on the network assumed by each core model, one core model would further be modified into 1, 3, 7 or 21 submodels.

In total, we implemented 164 models for four comparisons of the overall responses of species to climate warming and climate cooling (Supplementary Table 5) at different confidence levels to again assess the robustness of our main results (that is, those assessed without confidence level restrictions): (1) warming positive responses versus all remaining species, (2) warming negative species versus all remaining species, (3) species that exhibited overall sensitivity to climate warming or cooling (that is, warming positive + warming negative species) versus species with consistent N_e increases or decreases for both the climate warming and climate cooling responses and (4) species that exhibited consistently decreasing N_e versus all remaining species. For each comparison, PPA provides the number of independence claims made by the model, the number of parameters, the C statistic and the accompanying P value, where significance (at $P < 0.05$) indicates that the available evidence rejects the model (that is, the model does not provide a good fit to the data[58]). Thus, after discarding rejected models we calculated the top-ranked model (on the basis of $\Delta CICc$) and the average of the best-performing models ($\Delta CICc \leq 2$) for each comparison. Detailed results of the best-performing models for each confidence level are provided in Supplementary Tables 6–10, with

their associated directed acyclic graphs and regression coefficients provided in Supplementary Figs. 11–20.

Reporting summary

Further information on research design is available in the Nature Portfolio Reporting Summary linked to this article.

Data availability

All data underlying these analyses (including raw N_e estimates over time for each species) are available in the Dryad Digital Repository[38].

Code availability

All code underlying these analyses is available in the Dryad Digital Repository[38].

References

1. Butchart, S. H. M. et al. Global biodiversity: indicators of recent declines. *Science.* **328**, 1164–1168 (2010).
2. Dirzo, R. et al. Defaunation in the Anthropocene. *Science.* **345**, 401–406 (2014).
3. Intergovernmental Science-Policy Platform on Biodiversity and Ecosystem Services (IPBES). *Global Assessment Report on Biodiversity and Ecosystem Services* (IPBES secretariat, 2019).
4. Rosenberg, K. V. et al. Decline of the North American avifauna. *Science.* **366**, 120–124 (2019).
5. Fordham, D. A. et al. Using paleo-archives to safeguard biodiversity under climate change. *Science.* **369**, eabc5654 (2020).
6. Nogués-Bravo, D. et al. Cracking the code of biodiversity responses to past climate change. *Trends Ecol. Evol.* **33**, 765–776 (2018).
7. Foden, W. B. et al. Climate change vulnerability assessment of species. *WIREs Clim. Change.* **10**, e551 (2019).
8. Chattopadhyay, B., Garg, K. M., Ray, R. & Rheindt, F. E. Fluctuating fortunes: genomes and habitat reconstructions reveal global climate-mediated changes in bats' genetic diversity. *Proc. R. Soc. B.* **286**, 20190304 (2019).
9. Chen, L. et al. Large-scale ruminant genome sequencing provides insights into their evolution and distinct traits. *Science.* **364**, eaav6202 (2019).
10. Peart, C. R. et al. Determinants of genetic variation across eco-evolutionary scales in pinnipeds. *Nat. Ecol. Evol.* **4**, 1095–1104 (2020).
11. Jenouvrier, S. Impacts of climate change on avian populations. *Glob. Change Biol.* **19**, 2036–2057 (2013).
12. Pacifici, M. et al. Species' traits influenced their response to recent climate change. *Nat. Clim. Change.* **7**, 205–208 (2017).
13. Foden, W. B. et al. Identifying the world's most climate change vulnerable species: a systematic trait-based assessment of all birds, amphibians and corals. *PLoS ONE.* **8**, e65427 (2013).
14. Telenský, T., Klvaňa, P., Jelínek, M., Cepák, J. & Reif, J. The influence of climate variability on demographic rates of avian Afro-palearctic migrants. *Sci. Rep.* **10**, 17592 (2020).
15. Jiguet, F., Gadot, A.-S., Julliard, R., Newson, S. E. & Couvet, D. Climate envelope, life history traits and the resilience of birds facing global change. *Glob. Change Biol.* **13**, 1672–1684 (2007).
16. Lorenzen, E. D. et al. Species-specific responses of Late Quaternary megafauna to climate and humans. *Nature.* **479**, 359–364 (2011).
17. Hung, C.-M. et al. Drastic population fluctuations explain the rapid extinction of the passenger pigeon. *Proc. Natl. Acad. Sci. USA.* **111**, 10636–10641 (2014).
18. Feng, S. et al. The genomic footprints of the fall and recovery of the crested ibis. *Curr. Biol.* **29**, 340–349.e7 (2019).
19. Feng, S. et al. Dense sampling of bird diversity increases power of comparative genomics. *Nature.* **587**, 252–257 (2020).
20. Li, H. & Durbin, R. Inference of human population history from individual whole-genome sequences. *Nature.* **475**, 493–496 (2011).
21. Fjeldså, J., Christidis, L. & Ericson, P. G. P. (eds) *The Largest Avian Radiation: The Evolution of Perching Birds, or the Order Passeriformes* (Lynx Edicions, 2020).
22. Bay, R. A. et al. Genomic signals of selection predict climate-driven population declines in a migratory bird. *Science.* **359**, 83–86 (2018).
23. Parmesan, C. Ecological and evolutionary responses to recent climate change. *Annu. Rev. Ecol. Evol. Syst.* **37**, 637–669 (2006).
24. Angert, A. L. et al. Do species' traits predict recent shifts at expanding range edges? *Ecol. Lett.* **14**, 677–689 (2011).
25. McCain, C. M. & King, S. R. B. Body size and activity times mediate mammalian responses to climate change. *Glob. Change Biol.* **20**, 1760–1769 (2014).
26. Barrett, R. D. H. & Schluter, D. Adaptation from standing genetic variation. *Trends Ecol. Evol.* **23**, 38–44 (2008).
27. Hancock, A. M. et al. Adaptation to climate across the Arabidopsis thaliana genome. *Science.* **334**, 83–86 (2011).
28. McKenna, A. et al. The Genome Analysis Toolkit: a MapReduce framework for analyzing next-generation DNA sequencing data. *Genome Res.* **20**, 1297–1303 (2010).
29. Nadachowska-Brzyska, K., Li, C., Smeds, L., Zhang, G. & Ellegren, H. Temporal dynamics of avian populations during pleistocene revealed by whole-genome sequences. *Curr. Biol.* **25**, 1375–1380 (2015).
30. Jarvis, E. D. et al. Whole-genome analyses resolve early branches in the tree of life of modern birds. *Science.* **346**, 1320–1331 (2014).
31. Rokas, A., Williams, B. L., King, N. & Carroll, S. B. Genome-scale approaches to resolving incongruence in molecular phylogenies. *Nature.* **425**, 798–804 (2003).
32. Wolf, Y. I., Rogozin, I. B., Grishin, N. V. & Koonin, E. V. Genome trees and the tree of life. *Trends Genet.* **18**, 472–479 (2002).
33. Yang, Z. PAML: a program package for phylogenetic analysis by maximum likelihood. *Comput. Appl. Biosci.* **13**, 555–556 (1997).
34. Forest, F. Calibrating the tree of life: fossils, molecules and evolutionary timescales. *Ann. Bot.* **104**, 789–794 (2009).
35. Magallón, S. A. Dating lineages: molecular and paleontological approaches to the temporal framework of clades. *Int. J. Plant Sci.* **165**, S7–S21 (2004).
36. Nadachowska-Brzyska, K., Burri, R., Smeds, L. & Ellegren, H. PSMC analysis of effective population sizes in molecular ecology and its application to black-and-white Ficedula flycatchers. *Mol. Ecol.* **25**, 1058–1072 (2016).
37. Bird, J. P. et al. Generation lengths of the world's birds and their implications for extinction risk. *Cons. Biol.* **34**, 1252–1261 (2020).
38. Germain, R. et al. Species-specific traits mediate avian demographic responses under past climate change. Preprint at http://datadryad.org/stash/dataset/doi:10.5061/dryad.fn2z34tz8 (2022).
39. Patton, A. H. et al. Contemporary demographic reconstruction methods are robust to genome assembly quality: a case study in Tasmanian devils. *Mol. Biol. Evol.* **36**, 2906–2921 (2019).
40. Liu, X. & Fu, Y.-X. Exploring population size changes using SNP frequency spectra. *Nat. Genet.* **47**, 555–559 (2015).
41. Terhorst, J. & Song, Y. S. Fundamental limits on the accuracy of demographic inference based on the sample frequency spectrum. *Proc. Natl Acad. Sci. USA* **112**, 7677–7682 (2015).
42. Terhorst, J., Kamm, J. A. & Song, Y. S. Robust and scalable inference of population history from hundreds of unphased whole genomes. *Nat. Genet.* **49**, 303–309 (2017).
43. Lapierre, M., Lambert, A. & Achaz, G. Accuracy of demographic inferences from the site frequency spectrum: the case of the yoruba population. *Genetics.* **206**, 439–449 (2017).

44. Mazet, O., Rodríguez, W., Grusea, S., Boitard, S. & Chikhi, L. On the importance of being structured: instantaneous coalescence rates and human evolution—lessons for ancestral population size inference? *Heredity.* **116**, 362–371 (2016).

45. Chikhi, L. et al. The IICR (inverse instantaneous coalescence rate) as a summary of genomic diversity: insights into demographic inference and model choice. *Heredity.* **120**, 13–24 (2018).

46. Teixeira, H. et al. Impact of model assumptions on demographic inferences: the case study of two sympatric mouse lemurs in northwestern Madagascar. *BMC Ecol. Evol.* **21**, 197 (2021).

47. Galili, T. dendextend: an R package for visualizing, adjusting and comparing trees of hierarchical clustering. *Bioinformatics.* **31**, 3718–3720 (2015).

48. Smith, M. R. TreeDist: distances between phylogenetic trees. *Zenodo* https://doi.org/10.5281/ZENODO.3528124 (2019).

49. Paleo-López, R. et al. A phylogenetic analysis of macroevolutionary patterns in fermentative yeasts. *Ecol. Evol.* **6**, 3851–3861 (2016).

50. Snyder, C. W. Evolution of global temperature over the past two million years. *Nature.* **538**, 226–228 (2016).

51. David, F. N. *Tables of the Ordinates and Probability Integral of the Distribution of the Correlation Coefficient in Small Samples* (Cambridge Univ. Press, 1938).

52. Guenther, W. C. Desk calculation of probabilities for the distribution of the sample correlation coefficient. *Am. Stat.* **31**, 45–48 (1977).

53. Bates, D., Mächler, M., Bolker, B. & Walker, S. Fitting linear mixed-effects models using lme4. *J. Stat. Softw.* **67**, 1–48 (2015).

54. Barton, K. MuMIn: multi-model inference. *R* (2022).

55. White, G. & Burnham, K. Program MARK: survival estimation from populations of marked animals. *Bird Study.* **46**, 120–139 (1999).

56. Nakagawa, S. & Schielzeth, H. A general and simple method for obtaining R2 from generalized linear mixed-effects models. *Methods Ecol. Evol.* **4**, 133–142 (2013).

57. van der Bijl, W. phylopath: perform phylogenetic path analysis. *R* (2021).

58. Gonzalez-Voyer, A. & von Hardenberg, A. in *Modern Phylogenetic Comparative Methods and Their Application in Evolutionary Biology* (ed Garamszegi, L.), pp 201–229 (Springer, 2014).

59. Holt, B. G. et al. An update of Wallace's zoogeographic regions of the world. *Science.* **339**, 74–78 (2013).

Acknowledgements

Author contributions

Competing interests

The authors declare no competing interests.

Additional information

Supplementary information The online version contains supplementary material available at https://doi.org/10.1038/s41559-023-02055-3.

Correspondence and requests for materials should be addressed to Ryan R. Germain, Guojie Zhang or David Nogués-Bravo.

Peer review information *Nature Ecology & Evolution* thanks Nicolas Dussex and the other, anonymous, reviewer(s) for their contribution to the peer review of this work.

Reprints and permissions information is available at www.nature.com/reprints.

Corresponding author(s): Ryan Germain, David Nogues-Bravo, Guojie Zhang

Last updated by author(s): 21/03/2023

Reporting Summary

Nature Portfolio wishes to improve the reproducibility of the work that we publish. This form provides structure for consistency and transparency in reporting. For further information on Nature Portfolio policies, see our Editorial Policies and the Editorial Policy Checklist.

Statistics

For all statistical analyses, confirm that the following items are present in the figure legend, table legend, main text, or Methods section.

n/a	Confirmed	
☐	☒	The exact sample size (*n*) for each experimental group/condition, given as a discrete number and unit of measurement
☐	☒	A statement on whether measurements were taken from distinct samples or whether the same sample was measured repeatedly
☐	☒	The statistical test(s) used AND whether they are one- or two-sided *Only common tests should be described solely by name; describe more complex techniques in the Methods section.*
☐	☒	A description of all covariates tested
☐	☒	A description of any assumptions or corrections, such as tests of normality and adjustment for multiple comparisons
☐	☒	A full description of the statistical parameters including central tendency (e.g. means) or other basic estimates (e.g. regression coefficient) AND variation (e.g. standard deviation) or associated estimates of uncertainty (e.g. confidence intervals)
☐	☒	For null hypothesis testing, the test statistic (e.g. F, t, r) with confidence intervals, effect sizes, degrees of freedom and P value noted *Give P values as exact values whenever suitable.*
☒	☐	For Bayesian analysis, information on the choice of priors and Markov chain Monte Carlo settings
☐	☒	For hierarchical and complex designs, identification of the appropriate level for tests and full reporting of outcomes
☐	☒	Estimates of effect sizes (e.g. Cohen's *d*, Pearson's *r*), indicating how they were calculated

Our web collection on statistics for biologists contains articles on many of the points above.

Software and code

Policy information about availability of computer code

Data collection	No software was used in data collection
Data analysis	All analyses were completed using R version 3.6.3

For manuscripts utilizing custom algorithms or software that are central to the research but not yet described in published literature, software must be made available to editors and reviewers. We strongly encourage code deposition in a community repository (e.g. GitHub). See the Nature Portfolio guidelines for submitting code & software for further information.

Data

Policy information about availability of data

All manuscripts must include a data availability statement. This statement should provide the following information, where applicable:
- Accession codes, unique identifiers, or web links for publicly available datasets
- A description of any restrictions on data availability
- For clinical datasets or third party data, please ensure that the statement adheres to our policy

All data and underlying these analyses (including raw Ne estimates over time for each species) are available in the Dryad Digital Repository (http://datadryad.org/stash/dataset/doi:10.5061/dryad.fn2z34tz8)

Human research participants

Policy information about [studies involving human research participants and Sex and Gender in Research.](#)

Reporting on sex and gender	This study did not include human participants
Population characteristics	This study did not include human participants
Recruitment	This study did not include human participants
Ethics oversight	This study did not include human participants

Note that full information on the approval of the study protocol must also be provided in the manuscript.

Field-specific reporting

Please select the one below that is the best fit for your research. If you are not sure, read the appropriate sections before making your selection.

☐ Life sciences   ☐ Behavioural & social sciences   ☒ Ecological, evolutionary & environmental sciences

For a reference copy of the document with all sections, see [nature.com/documents/nr-reporting-summary-flat.pdf](#)

Ecological, evolutionary & environmental sciences study design

All studies must disclose on these points even when the disclosure is negative.

Study description	This study uses whole-genome sequence data from 263 bird species to estimate changes in effective population size over the past million years and evaluates the role of 6 key morphological/life-history traits on population responses during climate warming and cooling
Research sample	This study builds upon whole-genome sequence data for 263 bird species previously published by Feng et al (2020; Nature 587, 252–257), which represents broad geographic and taxonomic coverage of the world's birds
Sampling strategy	From an original list of 345 bird species (see Table S1), genomic estimates of Ne from 263 species passed all quality control checks and contain information for full demographic estimates during the sample period of 30,000 – 1 million years ago
Data collection	Genomic data were assembled as part of the B10k Genomes project (https://b10k.genomics.cn/) following standardized protocols (Feng et al. 2022 Nature 587, 252–257). Morphological/life-history data were assembled by J. Tobias as part of the Avonet trait database following standardized protocols (Tobias et al. 2022 Ecol Lett 25, 581-597)
Timing and spatial scale	Whole genome sequence data were collected beginning in 2014 as part of the B10k Genomes project Phase 1 (https://b10k.genomics.cn/), and ended in 2021 with the completion of Phase 2 (Feng et al. 2022 Nature 587, 252–257). Species included in our study represent the full global extent of the world's birds (excluding Antarctica), with the number of species sampled from each of the Earth's major zoogeographic realms presented in Figure 3
Data exclusions	Of 345 species for which whole genome sequence data were initially generated, 82 were excluded following pre-established criteria (Nadachowska-Brzyska et al 2015, Curr. Biol. 25, 1375–1380) or if demographic data did not cover the full extend of the focal study period (30,000 years – 1 million years ago). Full details of all exclusions are provided in the Methods section.
Reproducibility	No experiments were included in this manuscript
Randomization	Species were allocated to groups based on their demographic responses to period of climate warming/cooling. However, each group was analyzed separately to determine the effects of key morphological/life-history traits on different long-term demographic responses. Groups were not directly compared, and thus randomization was not applicable for this study.
Blinding	Our study does not include experiments or comparisons across groups, and thus blinding was not necessary. Despite this, all analyses were conducted with species names replaced by alpha-numeric codes (as part of data organization within the B10k genomes project), and species names were re-inserted at the writing phase of the project.

Did the study involve field work?   ☐ Yes   ☒ No

Reporting for specific materials, systems and methods

We require information from authors about some types of materials, experimental systems and methods used in many studies. Here, indicate whether each material, system or method listed is relevant to your study. If you are not sure if a list item applies to your research, read the appropriate section before selecting a response.

Materials & experimental systems

n/a	Involved in the study
☒ ☐	Antibodies
☒ ☐	Eukaryotic cell lines
☒ ☐	Palaeontology and archaeology
☒ ☐	Animals and other organisms
☒ ☐	Clinical data
☒ ☐	Dual use research of concern

Methods

n/a	Involved in the study
☒ ☐	ChIP-seq
☒ ☐	Flow cytometry
☒ ☐	MRI-based neuroimaging